AIAA 82-4222

Unsteady Aerodynamics and Motions of the Pioneer Venus Probes

Alvin Seiff* and Charles E. DeRose†
NASA Ames Research Center, Edwards, Calif.
and
Vincent U. Muirhead‡
University of Kansas, Lawrence, Kansas

Helicopter drop tests were made of models of the Pioneer Venus probe descent configurations to characterize their unsteady forces and angular dynamics in equilibrium descent. The axial and normal forces were found to be unsteady in magnitude by about 10 and 5% of the mean axial force, respectively. A cycle of the axial variation takes place in flight distances of from 15 to 40 diameters. The unsteadiness almost certainly is associated with the wake. Angular motions which do not converge to zero angle of attack even in very long duration descent are excited by the unsteady pitching moments. The nearly spherical large probe model was aerodynamically more unsteady than the round-nosed conical small probe model. Data returned from Venus by the Pioneer Venus probes show unsteady axial forces and angular motions similar to those seen in the drop tests.

Nomenclature

$a_{x,y,z}$ = accelerations in the three, body fixed coordinate directions, m/s^2
a_D = drag deceleration, along the flight path, m/s^2
a_N = resultant acceleration normal to the body axis of symmetry, m/s^2
A = reference area = $\pi d^2/4$, m^2
C_A = axial force coefficient
cg = center of gravity
C_D = drag coefficient
C_{m_α} = pitching moment curve slope, per radian
C_N = normal force coefficient
d = reference dimension, largest base dimeter, m
D = drag force, n
g or g_E = gravitational acceleration on Earth = 9.81 m/s^2 at mean surface
g_V = gravitational acceleration Venus = 8.87 m/s^2 at mean surface
I_y = moment of inertia about a transverse axis through the cg, kg m^2
k = reciprocal of relaxation distance for model to acquire V_t, m^{-1}
M = Mach number
m = probe or model mass, kg
Re = Reynolds number based on frontal diameter
t = time, s
T = period of oscillation, s
V = drop velocity, m/s
V_t = terminal or equilibrium descent velocity, m/s
W = probe or model weight, n
x,y,z = coordinates fixed in probe or model with z along axis of symmetry, m
Z = altitude, km
α = angle of attack (in x-z plane), deg
α_r = resultant angle of attack (in plane of a_N), deg
β = angle of sideslip (in y-z plane), deg
ρ = atmospheric density, kg/m^3

Received Aug. 7, 1981; revision received March 8, 1982. This paper is declared a work of the U.S. Government and therefore is in the public domain.

*Senior Staff Scientist, Space Science Division. Associate Fellow AIAA.
†Aerospace Engineer, Thermo and Gas Dynamics Division.
‡Chairman, Department of Aerospace Engineering. Member AIAA.

Introduction

WELL before the launch of the four Pioneer Venus probes in August 1978, the Atmosphere Structure Experiment team had identified probe aerodynamic buffeting at subsonic speeds as a significant noise background for the measurement of probe lateral and axial accelerations in the hour-long descent period. Probe accelerations were to be measured at Venus to define the structure of the upper atmosphere during high speed entry, and to reconstruct the descent trajectory, define vertical flow velocities, and search for evidence of wave motions and turbulence.[1] The noise background was recognized to be a degrading influence, so it was decided to: a) see if it could be reduced, which led to the work reported in Refs. 2 and 3; and b) characterize it from drop tests in the Earth's atmosphere, so that the known signature would not be misinterpreted as due to Venus atmospheric phenomena. This led to the work reported herein.

For purposes of the Venus experiments, the ideal level of buffeting was, of course, zero. Realistically, the goal was to reduce it to the lowest attainable level, but definitely below the level of the first turbulence counting threshold, which was set at $\pm 0.05 g_E$. The buffeting arises from the inherent unsteadiness of the wake and base pressure forces of blunt bodies. It is most prominent subsonically because base pressure forces can be comparable to those on the forebody at low speeds. The unsteady pressures give rise to aerodynamic pitching moments as well, and hence apply somewhat random inputs to the probe angular motions.

Spherical bodies are well known to be subject to effects of unsteady base pressures which can, e.g., produce erratic flight of nonspinning baseballs and balloons. The Pioneer Venus large probe was basically spherical (Fig. 1a), but had a flat based ramp around its middle to fix the line of separation of the wake. The Pioneer Venus small probes (Fig. 1b) were round-nosed 45-deg half-angle cones, also with a well-fixed wake separation line. Prior experience in the Planetary Atmosphere Experiments Test (PAET) had indicated significant buffeting, evidenced by unsteadiness in the measured ac-

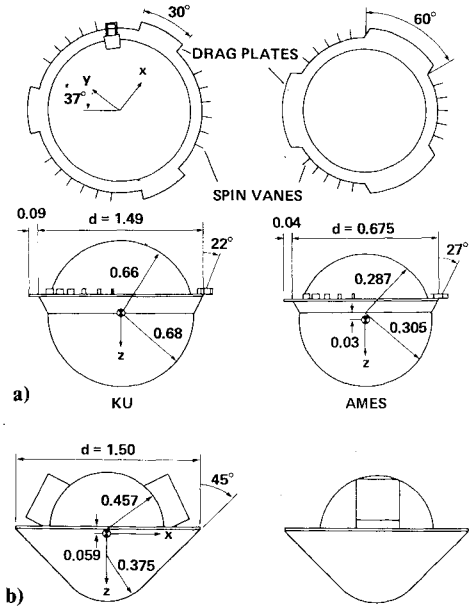

Fig. 1 Drawings of the drop models. Dimensions are in meters. a) Large probe: model masses were 66.9 kg (KU) and 17.6 kg (Ames); estimated $I_Y = 22.7$ kg m^2 (KU); proturberance on back of KU model simulates cloud particle spectrometer. b) Small probe: mass = 73.9 kg, $I_y = 19.1$ kg m^2 (estimated).

celerations of approximately $\pm 0.05g$, both laterally and axially.[4]

The drop tests of Pioneer Venus models began at Ames Research Center in 1974 with a test of a large probe model. At this time, the configuration was not yet firm in all details. A small scale model with the geometry shown at the right in Fig. 1a and labeled "Ames" was dropped from a helicopter at relatively low altitude (500 m) at a Reynolds number of 1.4 million. Since Venus probe Reynolds numbers in descent were estimated to range from 7 to 20 million, and base flows depend on Reynolds number, a test at higher Reynolds number was desired. A test of the small probe configuration was also needed. Therefore tests at the University of Kansas (KU) were undertaken, designed to achieve a higher Reynolds number within the constraints of practicality and cost. Models used in these tests are sketched at the left in Fig. 1a and in 1b. These tests were made from a much higher drop altitude, 2800 m above impact, to provide a longer observing time, and with increased instrumentation.

This paper reports and analyzes the results of these tests. It also compares them with acceleration data returned from the actual Pioneer Venus probes in descent, to reach conclusions relative to unsteady aerodynamics and probe dynamics experienced in the Venus descents.

Models, Instrumentation, and Test Procedure

Drawings of three drop models are shown in Fig. 1. The large probe models (Fig. 1a) represent a spherical pressure vessel with a separate, slightly larger radius forebody fairing which terminates in the separation ramp, as designed by the probe contractor, Hughes Aerospace Company, El Segundo, Calif. Three drag plates were added at the ramp base to prolong slightly the descent time of the probe at Venus. Spin vanes were used to rotate the probe in descent, balance out aerodynamic asymmetry, and provide 360-deg sampling for some of the optical instruments. The drag plate sectors and ramp angles on the two large probe drop models differed, the Ames model having larger drag plates. The KU model simulates the final geometry, except that its spin vanes were set at 11 deg incidence, appreciably larger than the flight-selected value, 2.7 deg. The center of gravity of the KU model was very close to that selected for the Venus probe.

The small probe model (Fig. 1b) is basically a round-nosed cone with an afterbody of reduced radius, which fixes the wake separation line. This geometry simply results from the pressure vessel being nested behind the entry heat shield. Two instrument boxes on the afterbody housed deployable sensors on the Venus probes, a temperature sensor and pressure inlet in one, and a net flux radiometer in the other. These sensors were deployed to positions outboard of the cone base in descent. On the drop models the width of these boxes simulates the deployed condition, with the lid open and rotated 180 deg from its closed position. The drop model center of gravity was very close to that of the Venus small probes.

Primary onboard instrumentation was a set of three-axis accelerometers (the same set was used in all three drops), and an analog telemetry transmitter. The accelerometers and transmitter were on a common mounting plate, located to place the accelerometers near the model center of gravity. The model shells were made of molded plastic filled with low density polyurethane foam to support the instrumentation and provide shock absorption on impact. Power was provided by five dry cell batteries distributed around the perimeter of the telemetry package. The ramp base and drag plates were a plywood ring, and the spin vanes were thin aluminum plates.

The accelerometers on all three probes were Systron Donner Model 4310 servo-rebalance accelerometers, with ranges from 0 to $1g$ in the z axis and $\pm 0.5g$ in the lateral axes. They are capable of accuracy better than 0.1% of full scale. The sensors were calibrated against the Earth's gravitational field just before each drop test. The data were recorded on magnetic tape and read out onto a strip chart recorder with a linear resolution of 0.36 g/cm. Readings from this chart accurate to ± 0.1 mm would correspond to $\pm 0.004g$. Because of probe oscillations on the helicopter prior to drop, the zero level on the chart was uncertain to $\sim 0.01g$.

The two KU models were additionally instrumented with temperature and pressure sensors to measure the ambient atmosphere during descent. These functioned well on the small probe model and gave insights into meteorological conditions encountered. The temperature and pressure sensors failed to return data on the large probe drop because of an electrical failure on the probe.

Drop altitude was determined from altimeters on the aircraft. Ambient atmospheric conditions were also measured during ascent for the drop by use of aircraft instruments. Models were supported from the helicopter landing gear by means of a short (0.5-m) nylon strap in the KU drops, and released on ground command. In the Ames drop, a longer (15-m) steel support cable was used with release controlled by the helicopter crew. Telemetry receivers and magnetic tape recorders were located nearby the drop sites. The KU drops were made at Fort Riley, Kansas over a gunnery range. Elevation of the landing site was 408 m above sea level. Weather conditions for these drops were cloudy, with atmospheric temperatures near the surface of 16.5 and 22°C for the small and large probe tests. Drop dates were June 15, 1977 and August 3, 1977, respectively. The Ames drop was made just outside Ames Research Center, over an open field, at an elevation < 10 m above sea level. The helicopter altimeter was zeroed for this drop at the landing site before takeoff. The drop was made under a clear sky on November 26, 1974, with an ambient temperature of about 15°C.

Test Data

A representative section of the accelerometer record of the three components of aerodynamic acceleration experienced by the small probe model late in the drop period is shown in Fig. 2. Corresponding data for the KU large probe model are given in Fig. 3. Total drop times were 83 s (small probe) and 81.5 s (large probe). The altitude range above impact represented in these figures is from about 700 to 85 m (small probe) and 678 to 50 m (large probe). Equilibrium velocities in these data segments were around 30 m/s, corresponding to a Mach number of 0.09. Reynolds numbers based on freestream

properties and maximum frontal diameter were $\sim 2.8 \times 10^6$.

Unsteadiness is evident in all three components of the aerodynamic force for both models, but in the x and y axes, it partly reflects angular motions and the development of normal forces at angles of attack and sideslip. In the z axis, for small angular motions, it is almost purely a result of unsteadiness in the axial force, and we will examine this component first. Then we will return to consider the interpretation of the x- and y-axis data.

The unsteady amplitude of a_z is comparable for the two configurations, but the frequency content differs, the large probe model generating higher frequencies. The amplitudes and representative periods from the two a_z records are summarized in Table 1.

The period estimates were made by noting time intervals from peak to peak and neglecting the minor contribution of the highest frequency component which, for the large probe, has a period of ~ 0.1 s. The dimensionless Strouhal period, VT/d, is listed in the last column for each model. It represents the distance flown from one acceleration peak to the next expressed in diameters, and is typically ~ 20. During the initial 20 s of the large probe record (not shown), the variation in acceleration is dominated by large attitude excursions, and hence is not representative of unsteady aerodynamic behavior. It was therefore omitted from Table 1. The extreme range of the variation is ± 1.05 m/s^2 ($\pm 10.5\%$) for the small probe, and ± 1.1 m/s^2 ($\pm 11\%$) for the large probe, a very sizable unsteadiness. Note that the zero axis is not suppressed in these plots.

In the lateral axes, the small probe data show approximate symmetry about the zero axes and a representative amplitude of 0.5 m/s^2. There is evidence throughout the record, seen in Fig. 2 between 69 and 80 s, of a near-sinusoidal component with a period ~ 2.2 s, with a noise component superimposed. The noise component has a typical period of from 0.3 to 0.4 s.

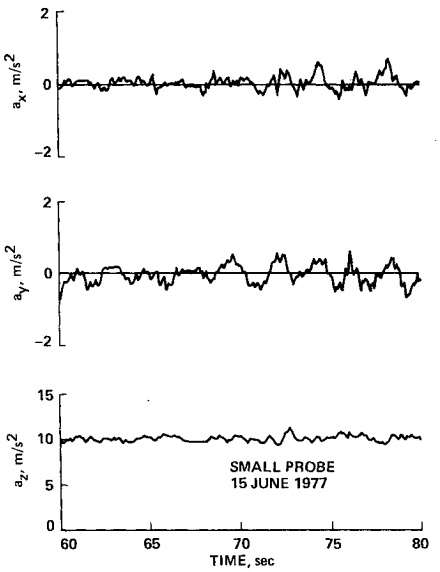

Fig. 2 Three-axis accelerometer data from the small probe model drop, for 20 s just above impact.

The regular oscillation amplitude increased near impact, starting at $t \sim 69$ s (altitude ~ 200 m).

The lateral components of the large probe acceleration are not symmetrical about the zero axes, and have an amplitude about the mean $\sim \pm 1$ m/s^2. The nearly sinusoidal component has a period near 1 s. The noise component has a period of from 0.1 to 0.3 s ($VT/d \sim 2$-6).

We will interpret the regular component of the lateral force oscillations as being associated with probe motions, while the random component is associated with buffeting or wake flow unsteadiness. The latter, of course, influences the former.

Data from the Ames drop test of the large probe model are shown in Fig. 4. Because of the lower drop altitude, the total drop time is only 17 s, and is shown. For almost half this time, the axial aerodynamic acceleration was increasing toward 1g, its value in equilibrium descent. Drop velocity at equilibrium was comparable to that for the larger KU models, 31 m/s, giving $M = 0.09$ and $Re = 1.4 \times 10^6$.

From 9 to 17 s, the range of a_z/g is 0.925-1.110, or a variability of $\pm 9\%$. Peak to peak periods range from 0.5 to 0.7 s and VT/d from 22 to 31, which is comparable to the values in the early period of the KU drop. (Some differences would be expected, because of the differences in drag plate geometry and Reynolds number.) The lateral axis accelerations on this drop show the presence of a nearly planar

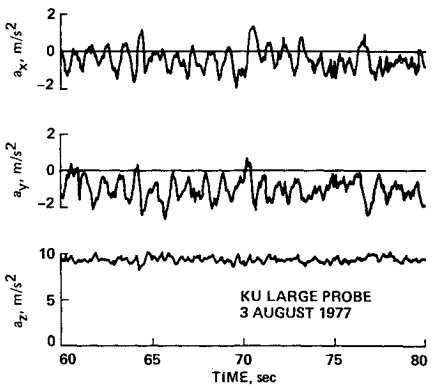

Fig. 3 20-s segment of the accelerometer data late in the descent of the KU large probe model.

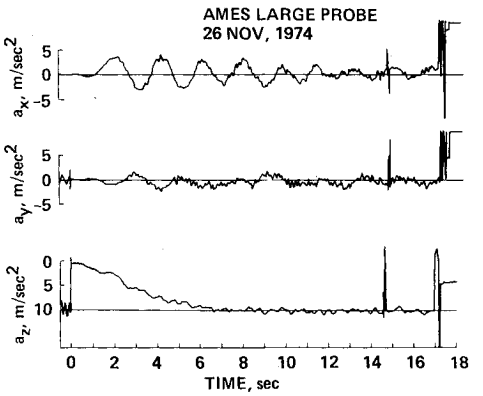

Fig. 4 The complete accelerometer data from the Ames large probe model drop.

Table 1 Summary of amplitudes and representative periods from the two a_z records

	Small probe				Large probe			
	a_z, m/s^2				a_z, m/s^2			
t, s	max	min	T, s	VT/d	max	min	T, s	VT/d
0-20	10.5	9.5	0.8-1.6	19-38	...	...	...	...
20-40	10.7	9.3	0.8-1.8	19-43	10.2	8.8	0.7-1.0	17-25
40-60	10.6	9.3	1.2	27	10.4	8.2	0.6-0.9	14-21
60-80	11.4	9.4	0.9-1.3	16-26	10.2	8.2	0.5-0.7	10-15

oscillation in the x-z plane, with $0.36g$ initial amplitude and fairly rapid convergence; it reaches half amplitude in 5 cycles. The random component of lateral acceleration (buffeting) is comparable in the two axes, and has a period of from 0.15 to 0.25 s (VT/d from 6 to 11). The lateral buffeting is of the order of 10% of the axial deceleration.

These data illustrate the nature and the magnitude of the unsteadiness of the aerodynamic forces on the Pioneer Venus probe geometries in low speed descent. This type of unsteadiness is not limited to these configurations but occurs quite generally with blunt bodies. It was, in fact, not possible to eliminate it by numerous geometrical variations on the Pioneer Venus large probe in wind tunnel tests, although some were found which could reduce it.[3] The best of these[2] was drop tested at Ames and found to be appreciably quieter in the axial component, with the low frequency component much suppressed, but was still not entirely free of unsteady accelerations.

In order to make further interpretations of the measured data, we analyzed the drop trajectories to define velocity and altitude histories, evaluated the effects of helicopter downwash and atmospheric motions, and interpreted the data to define the angular motions, as described in the following sections.

Trajectory Analysis

The transient period in which the model accelerates to terminal speed is governed by the equation

$$W-D=m\frac{dV}{dt} \tag{1}$$

$$\frac{dV}{dt}+\frac{C_DA}{2m}\rho V^2-g=0 \tag{2}$$

Restating Eq. (2) with altitude Z as independent variable gives

$$\frac{dV^2}{dZ}-kV^2+2g=0 \tag{3}$$

where

$$k=\rho\frac{C_DA}{m}$$

This may be integrated for the case where changes in ρ and C_D are small during the approach to terminal velocity V_t to obtain

$$V^2=(2g/k)\{1-\exp[-k(Z_i-Z)]\} \tag{4}$$

the equation defining the approach of V to V_t. Here, $1/k$ is the relaxation distance for approach of V^2 to within $1/e$ of V_t^2, e is the Naperian base, and Z_i is the initial, or drop altitude. From Eq. (4), the terminal velocity is a function of the ambient density,

$$V_t=(2g/k)^{1/2}=(2mg/C_DA_p)^{1/2} \tag{5}$$

The m/C_DA's of the three drop models were about 59.1 kg/m^2 (Ames large probe model), 54.0 kg/m^2 (KU large probe model), and 54.3 kg/m^2 (KU small probe model). The drag coefficients used in these m/C_DA's are 0.84, 0.71, and 0.77, respectively. The first of these was derived from the Ames drop test. The latter two were from wind tunnel tests.[5,6] At the mean altitudes, calculated terminal velocities are 31.1, 32.1, and 32.2 m/s, respectively. The calculated relaxation distances are 49, 53, and 53 m; at this drop distance $V^2=0.632\ V_t^2$, or $V=0.795\ V_t$. At twice this drop distance, $V=0.930\ V_t$, and at three times this drop distance (i.e., within ~150 m of drop altitude), $V=0.975\ V_t$.

By integration of the measured axial accelerations, we can compare measured drop trajectories with these somewhat idealized estimates. Idealizations include neglect of helicopter downwash effects; assumption of constant density and constant drag coefficient, i.e., no Reynolds number effect during acceleration from zero velocity, and no unsteadiness; and neglect of angle of attack effects. The integrations of measured accelerations also require assumptions, namely, that the angle of attack is known so that measured accelerations can be resolved to define the vertical component, and that the sensor calibration is exact.

Accelerometers in a free falling model measure only the aerodynamic accelerations, and not that due to gravitation. Thus the total vertical acceleration is the vector sum of the gravitational acceleration and the aerodynamic acceleration. For purely vertical motion,

$$\frac{dV}{dt}=g-a_D \tag{6}$$

where a_D is the drag deceleration. This is integrated to obtain

$$V(t)=gt-\int_0^t a_D dt \tag{7}$$

A second integration yields the altitude history of the drop. The velocity and altitude histories derived in this way and from the small probe pressure data are shown in Fig. 5 (small probe), Fig. 6 (KU large probe), and Fig. 7 (Ames large probe).

The KU accelerometer data were digitized for numerical integration with 20 samples/s. The Ames data were integrated by estimating mean values of a_D in 1 s intervals from the graphical data. Values of the accelerometer scale factor and zero level were slightly adjusted to make the drop altitude correspond to that measured by the helicopter altimeter within its uncertainty. In all cases, the aerodynamic accelerations were initially downward as indicated by an extended period (about 2 s) of $0g$ after model release. (The sensors read zero when input is negative.) Data on this transient period of the fall were thus incomplete. The downward acceleration resulted from helicopter downwash, estimated for the helicopter used in the KU drops to have a mean velocity of 15 m/s over the rotor disk. (This was estimated by setting the thrust of the helicopter rotor equal to the momentum flow in the downwash. Since thrust is equal and opposite to the helicopter weight, this gives $m_hg=\rho V_d^2A$, where m_h is the helicopter mass and V_d is the mean downwash velocity over the rotor disk. With $m_h=3425$ kg and rotor tip diameter = 14.6 m, $A=168$ m^2, and $V_d=14.8$ m/s at the drop altitude.) The initial level of V_t was established by the match of helicopter altitude at model release. On the small probe model, the measurements of atmospheric pressure permitted altitude and altitude rate to be independently determined. This is the altitude history shown in Fig. 5 and it closely supports that determined from acceleration data.

The velocity histories in the KU drops show fall velocities exceeding expected terminal velocities by as much as 8 m/s (Fig. 6). Beyond $t=70$ s, the small probe drop velocity is up to 3.3 m/s *less* than expected (Fig. 5). The velocity history of the Ames drop (Fig. 7) corresponds well to that predicted from

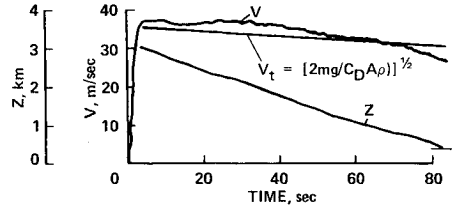

Fig. 5 Velocity and altitude histories of the small probe drop test. Velocity is from measured accelerations integrated in Eq. (7). Altitude is from pressures measured in descent. Terminal velocities expected from Eq. (5) are also shown.

Eqs. (4) and (5), both with respect to terminal velocity and the relaxation distance to acquire terminal velocity.

The observed velocity differences from those predicted can be explained by vertical motions of the atmosphere, drag coefficients differing from those selected, or errors in the data. For the small probe model, the drag coefficient was very well determined in wind tunnel tests and was supported by an analysis of the descent data of the three small probes on Venus.[7] In addition, as will be shown, the small probe model descended with small angles of attack. There were two gaps in the data caused by loss of telemetry signal, one from 18 to 24 s where the velocity hump originates. However, the velocity is generally a little high, starting at the time terminal velocity is first reached. We believe this is a result of the helicopter downwash, which remains significant (> 2 m/s) within a concentrated core of 30 or 40 m radius for several hundred meters below the helicopter.[8]

Below an altitude of 400 m from impact, the atmospheric motion implied is upflow. This is indicated in the velocity history by a terminal descent velocity less than that for a still atmosphere, and in the deceleration data by a period of average accelerations exceeding 10 m/s^2. The altitude history derived from the pressure data (Fig. 5) also shows a hump in this interval, suggesting upflow. We believe this model encountered the upflow in a convective cell near the surface, extending up to about 400 m above impact.

The large probe model velocity variation, Fig. 6, was initially well above the expected equilibrium descent velocity, but gradually approached it during the descent. We attribute this to a combination of helicopter downwash effect and the large amplitude of pitching oscillation, initially about 35 deg as we shall show in the following section. The drag coefficient of this model varies significantly with angle of attack, e.g., C_D at $\alpha = 30$ deg is about 84% of that at $\alpha = 0$ (Ref. 9). This can account for about half of the excess descent velocity, and helicopter downwash can account for the remainder. Both tend to diminish as the model moves away from the helicopter and the angle of attack disturbance converges. Near the ground, again, a limited region of upflow is indicated.

The close correspondence of velocities in the Ames drop to those expected probably reflects the use of a smaller helicopter and suggests that the model did not remain in the downwash core throughout its descent.

Angular Motions

The drop models receive some angular disturbance at release from the aircraft. Thereafter, the motion converges due to damping, and is continually reexcited by buffeting moments. The nature of the observed oscillations can indicate the relative importance of these effects, and the type of angular motion to be expected in equilibrium descent.

Angles of attack were derived from the lateral acceleration data and normal force coefficients measured in wind tunnels.[5,6,9] Ratios of a_N/a_z were used to enter graphs of C_N/C_A as a function of α to determine α. The wind tunnel data are shown in Fig. 8. For the large probe, data with both drag plate geometries were available. There is asymmetry in the data for plus and minus angles of attack because of the drag plate asymmetry. Data from two sources for the small probe geometry are in very close agreement. Perhaps surprisingly, the large probe develops about twice as much normal force at a given angle of attack as the small probe.

In the absence of unsteady side forces, this procedure for determining α would be rigorous, since the ratio of the normal force due to angle of attack to the axial force would indeed be equal to the ratio of normal to axial acceleration. When the axial and lateral forces are fluctuating due to unsteadiness in the wake, the indicated angle of attack may differ from the actual angle of attack. Since the lateral accelerations typically showed a regular, near-sinusoidal component with a random component superimposed, the indicated angles of attack will also show a regular component and a noise component. The noise component is not necessarily associated with real variations in angle.

To represent the angular motions in two dimensions, the α and β components were calculated independently from a_x/a_z and a_y/a_z, respectively. The data are presented as plots of α

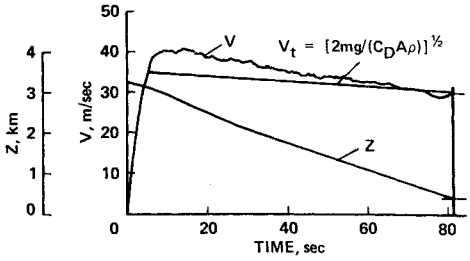

Fig. 6 Velocity and altitude histories of the KU large probe drop. Both are from integration of measured accelerations.

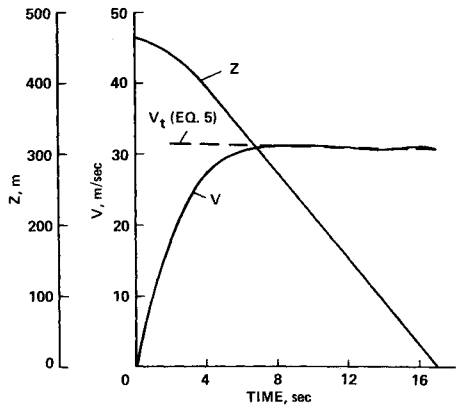

Fig. 7 Velocity and altitude histories, Ames large probe model, from measured accelerations.

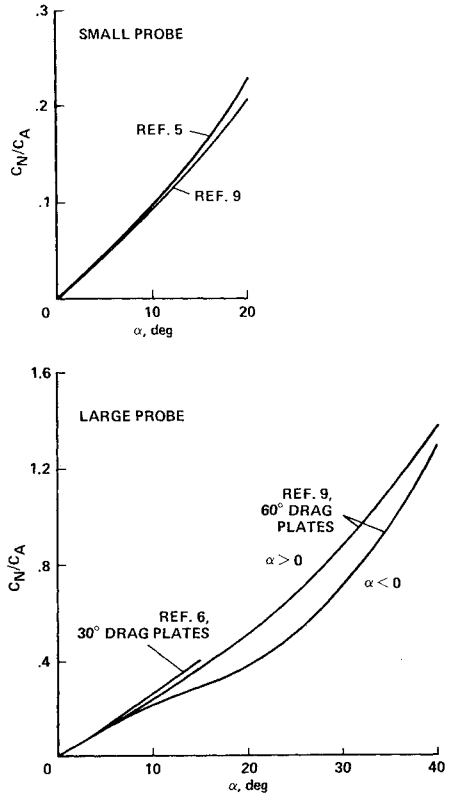

Fig. 8 Normal-to-axial force coefficient ratios from wind tunnel data.

vs β, and show the angular tracing of the model axis on a coordinate plane which rotates with the model. Two such graphs are shown in Fig. 9 for the small probe. In the early time period from 5 to 8 s, Fig. 9a, the indicated amplitude was about 9 deg, and the motion was close to the β plane, with some irregularity. Later in the drop, from 28 to 35 s (Fig. 9b), a relatively quiet period occurred, in which the peak lateral accelerations were 0.4 m/s. Motion amplitude is about 3 deg. After this quiet period, the motion grew again to a peak amplitude of 8 deg and a period of about 2 s. Starting at 70 s, amplitude growth was pronounced. In Fig. 5, it was at 70 s that the indication of convective upflow began. It is probable that this upflow is turbulent and that the increased pitching amplitude is excited by atmospheric turbulence. A peak amplitude of 10.7 deg was reached just before impact. The excitation of the model motions by turbulence is noteworthy. It is the counterpart of angular motions experienced by aircraft in turbulent atmospheres.

The natural frequency of the small probe model was estimated from wind tunnel[5] and ballistic range data on static stability (unpublished ballistic range data of DeRose) to be about 0.5 Hz, consistent with the 2-s period observed.

Two intervals in the KU large probe angular history are shown in Fig. 9c. The early motions were of very large amplitude and tend to be circular about the origin. In this interval, since no C_N/C_A data for 30-deg drag plates were available for $\alpha > 15$ deg, it was necessary to use data for the model with 60-deg drag plates, adjusted for the difference in initial slopes. (With 30-deg drag plates, the angles were about 0.8 as large as indicated by the mean curve for 60-deg drag plates.) The period was about 2.8 s early in the descent, decreasing to ~ 1 s as amplitude diminished. This indicates a nonlinear static stability, with the stability derivative increasing with decreasing amplitude. The early oscillations were large enough that they could be seen in the z-axis accelerations. The model was rolling at about 5 rpm, as determined by ground observers, who were also able to see the large amplitude spiraling motion. At 5 rpm, the model undergoes from 4 to 12 pitching cycles while rolling once, so that the rolling coordinates do not greatly distort the inertial pitching motion.

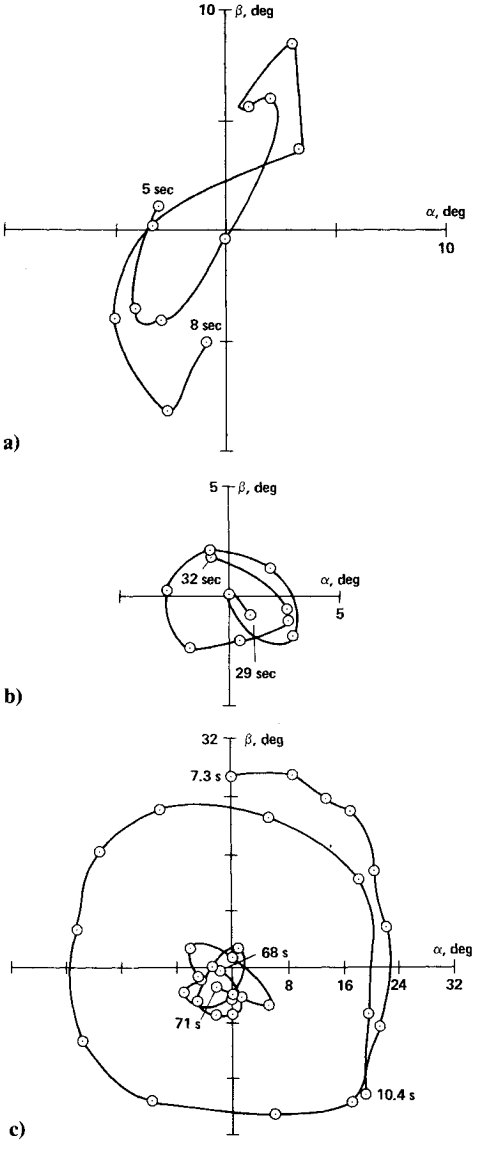

Fig. 9 Representative segments of the drop test model's angular motion histories: a) small probe, $t = 5$-8 s; b) small probe, $t = 29$-32 s; c) KU large probe.

Convergence of the oscillation was rapid. It decreased to half amplitude in about 20 s or 12 cycles. In the last 20 s, however, the motion had reached the level of ~ 8 deg peak amplitude (inner part, Fig. 9c) and was no longer damping rapidly, if at all. This amplitude and type of oscillation could be characteristic of the large probe model in steady-state descent, excited in large part by the unsteady aerodynamic moments.

The Ames large probe angular motions also started at very large amplitude, almost 50 deg and damped rapidly (half amplitude in one half-cycle). The motion was initially in a narrow elliptical figure rather than circular as in the KU drop. Over the last 6 s of the drop, motions in the α-β plane were erratic and peaked at about 8-deg amplitude, with no apparent tendency to decrease.

The KU large probe model exhibited much greater static stability in pitch and yaw than had been expected from wind tunnel measurements,[6] which predicted a static margin of $0.06d$ and $C_{m_\alpha} = -0.074$/rad. The stability observed in the drop test, based on the observed pitching frequency of 0.9 Hz at 10-deg pitching amplitude, was $C_{m_\alpha} = -0.65$/rad, which corresponds to a static margin of $0.59d$. In the data reduction, the moment curve slope is proportional to the model moment of inertia about a transverse axis through the cg, which was estimated, and could be uncertain by as much as 20%, leading to similar uncertainty in C_{m_α}. Since the centers of gravity in the drop test and in the Venus large probe almost coincided with the center of curvature of the spherical forebody and afterbody surfaces, pressure forces on these surfaces cannot contribute importantly to pitching moments. Thus the stability is largely associated with forces on the ramp, drag plates, and vanes. It follows that changes in the separated flow over the ramp and drag plate could strongly affect the stability. In the wind tunnel tests,[6] the margin of stability was, e.g., found to be increased by about 20% by installing spin vanes at 2.7 deg incidence. On the drop model, spin vane incidence was 11 deg. This, and differences in the flow separation geometry, could be responsible for the large increase in stability observed in the drop test.

Observations of Unsteady Aerodynamics from the Pioneer Probes at Venus

The four Pioneer Venus probes also carried accelerometers which sent data back to Earth on the aerodynamic accelerations sensed during the hour of descent through the lower atmosphere of Venus.[1] The descent Mach numbers of the small probes ranged from 0.18 at 50 km altitude to 0.02 at the surface, while their Reynolds numbers ranged from 3.6 to 12.4 million at the surface. The large probe jettisoned its parachute at 45 km altitude. In subsequent free fall, Mach numbers ranged from 0.17 to 0.026, with corresponding Reynolds numbers of from 6.9 to 19.5 million based on diameter of the ramp base. The large probe carried a three-axis accelerometer, while the small probes could accommodate only a single-axis sensor in the z axis.

The data rate which could be allocated to these measurements was limited, so data compression techniques were used. In the z axis, average accelerations taken over either 8- or 16-s intervals were telemetered to Earth. In addition, the number of excursions of the acceleration away from the nominal gravitational acceleration of Venus past preselected levels of nominally ± 0.055, ± 0.11, ± 0.22, and $\pm\ 0.33 g_V$ were counted. In the large probe lateral accelerometers, instantaneous samples were read every 16 s, as well as peak values in this sampling interval, and numbers of crossings of selected non-zero levels were counted in the x axis also.

The average acceleration data taken over 16-s intervals from an altitude of 26 km to impact of small probe 2, the day probe, are shown in Fig. 10. The altitude range is sufficient that changes in $g_V = -a_D$ are apparent, a consequence of decreasing distance to the center of Venus. The randomness of the samples is reduced by averaging over 16-s intervals but is still at the level of about $\pm 0.0022 g_V$.

Information on the amplitude and frequency of the fluctuations was derived from the level-crossing counters. Since the instrument scale factors differed from nominal, the levels were not symmetrically placed relative to the mean accelerations. On small probe 3, the night probe, e.g., one counting level fell just $\sim 0.01 g_V$ above the mean deceleration, thus measuring all deviations of a_z from the mean $> 0.01 g_V$. This level saw typically 25 crossings (a_z increasing) per 32-s data sample in the altitude range from 30 to 40 km. The mean period was thus 1.28 s, and the dimensionless Strouhal period, VT/d, ranged from 53 at 40 km to 34 at 30 km, comparable to the higher values from the small probe drop test, Table 1. (Since the counting level was very close to the mean acceleration, it is likely that it would record a larger number of counts than would be obtained by the procedure used in analyzing Fig. 2, where the period was defined by the time between major peaks.) In the Venus data, the counting rate decreased with probe altitude, with the mean period increasing to 2.0 s near the planet surface, while probe velocity was decreasing fourfold, from 32 to 8 m/s. Thus the Strouhal period decreased to a final value of 23, which is within the range of values seen in the drop test. The Strouhal periods in Venus descent were thus tending to decrease with altitude. While the cause of this decrease cannot be conclusively identified, it occurred as the Reynolds number increased from 5×10^6 to 13×10^6.

The next counting level was $0.06 g_V$ above the mean deceleration for this probe, and relatively few counts were obtained at this level, between 0 and 4 in 32-s samples from 48 km altitude to the surface. Hence excursions this large occurred every 16 s on the average, and most of the variation in a_z was smaller than $+0.06 g_V$. The next level below the mean deceleration was at $-0.10 g_V$, and only a few counts were recorded there, six in the entire descent. Hence the small probe buffet amplitude was typically less than $0.06 g_V$ and rarely reached $0.1 g_V$. This amplitude may be somewhat less than was observed in the drop tests, where the 20-s sample shown in Fig. 2 contains seven crossings of $+0.06\ g_E$ and one crossing of $0.10 g_E$ (none of $-0.1 g_E$). These data from small probe 3 are generally consistent with those from the other two small probes.

The instantaneous data on lateral axis accelerations of the large probe in descent on Venus were analyzed to define the indicated angles of attack in free fall after parachute release. The inferred resultant angles of attack are plotted in Fig. 11 against time with an auxiliary altitude scale. The randomness of the data is due to random timing of the samples relative to motion histories similar to those in Fig. 9. Thus the phase of each sample is arbitrary. The randomness is not scatter and does not reflect measurement uncertainty. The period of the pitching oscillation for the large probe on Venus was estimated to be 1.1 s, based on drop test stability observations. Thus, in recording one instantaneous sample every

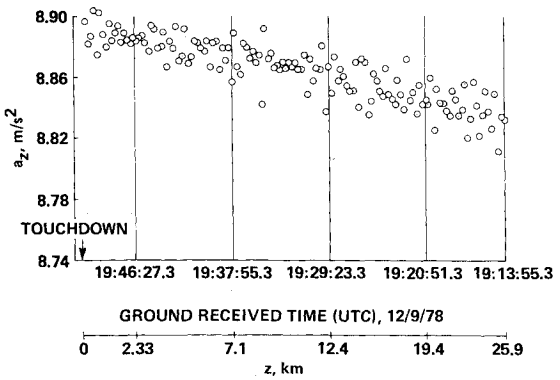

Fig. 10 Mean axial accelerations measured over 16-s intervals of the Pioneer Venus day probe (small probe 2) descent below 26 km in the atmosphere of Venus.

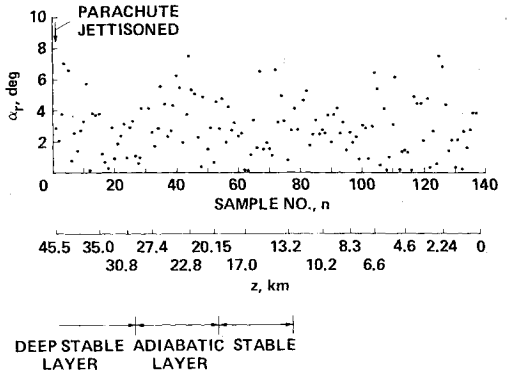

Fig. 11 Instantaneous random samples at 16-s intervals of the resultant angles of attack of the Pioneer Venus large probe descending in free fall below 45 km altitude in the atmosphere of Venus.

16 s, we are seeing one point on about every 15th cycle of oscillation. The upper and lower envelopes of the data should approximate maximum and minimum resultant angles which occurred. Thus, for sinusoidal planar oscillations, there is a 32% probability that a single sample will measure an angle of 7/8 peak amplitude or greater, and one data point in three should fall at or above 7/8 peak amplitude. Similarly, there is an 8% probability that a single sample will fall at less than 1/8 peak amplitude, and one data point in 12 should occur in this range. Hence the number of samples taken should have been adequate to indicate both the peak and minimum amplitudes.

Angles calculated from the data range from 0 to 8 deg, consistent with the KU drop test amplitudes at late times in the drop (Fig. 9c). In addition, there appears to be a correlation with the atmospheric stability against overturning, as indicated by temperature lapse rates. From 45 to 30 km, the atmospheric lapse rates were stable, indicating the absence of convective overturning.[1] In this interval, the envelope of the observed angles was decreasing from 7 to 3 deg. From 20 to 30 km altitude, the temperature data showed an adiabatic lapse rate, implying convective overturning and probably turbulence. In this layer, the amplitude increased again to 7.5 deg, and there were fewer random samples found in the vicinity of the origin, below about 2 deg, implying nonplanar motions. Below 20 km, the temperature data imply another stable, nonturbulent layer, and amplitude converges again. Below 13 km, there were no temperature lapse rate determinations, but the angle of attack data in Fig. 11 shows peak amplitudes < 4 deg from 12 to 7 km followed by larger amplitudes, up to 7.5 deg, between 6.6 and 2.2 km. This may imply a convective layer near the surface, but horizontal wind gusts could also produce a similar result. Reported wind measurements show variable direction in the deep atmosphere, perhaps implying gustiness.[10]

Concluding Remarks

These data illustrate the magnitude and character of the unsteady aerodynamic forces and moments which are experienced by blunt probes such as the Pioneer Venus probes in low speed equilibrium descent. Axial force unsteadiness can be surprisingly large, as much as $\pm 10\%$ of the drag. The dimensionless period of this variation corresponds to about 20 model diameters of flight. Lateral force unsteadiness is about half as great as the axial. It is blended with lateral axis accelerations due to normal force at angle of attack.

Because of random aerodynamic moments, the motions of these bodies do not converge to zero angle of attack, but undergo somewhat irregular oscillations even after very long fall times. Angles of attack are also excited in real atmospheres by turbulence and gusts. An excellent example of this was seen in the drop test of the small probe, which encountered a convective layer near the ground. This slowed the descent rate and increased pitching amplitude to ~ 10 deg.

The large probe configuration, basically a sphere, is more unsteady than the round-nosed 45-deg cone geometry of the small probe. Axial unsteadiness of the two bodies is comparable in magnitude, but of higher frequency on the large probe. The higher frequencies may be a result of discharge of small scale eddies off the three-dimensional drag plates, at a smaller scale than those of the basic body, because the scale of eddies is roughly proportional to the scale of the body discharging them.

The angular motion of the large probe is of larger amplitude and more irregular in equilibrium descent than that of the small probe. An equilibrium amplitude of ~ 8 deg occurs with the large probe compared to 4 deg for the small probe during quiet periods of the drop tests.

The probes in Venus descent behaved very similarly to the drop models. They were at higher Reynolds numbers by factors of from 2 to 6. The small probes on Venus showed Strouhal periods of from 23 to 53, somewhat larger than the range of values (16-43) seen in the drop tests. The differences could be partly a result of differences in measuring technique between the drop tests and the Venus data. The axial buffeting amplitude of the small probes was somewhat smaller on Venus than in the drop test, typically $<0.06g_V$ compared to peak amplitudes $<0.1g$ in the drop tests. There is no definite identification of the cause of these differences.

Angular motions of the large probe on Venus ranged up to 8 deg and thus were comparable to those in the drop test near the ground. Pitching amplitude seems to have been responsive to atmospheric conditions encountered on Venus. Amplitude converged to about 3 deg in the deep stable layer after parachute release, grew in the convective layer below the stable layer, and damped again in the lower stable layer. Near the surface, angular motions appeared to be responding to gusts which are indicated by wind data derived from radio tracking of the probes.

The large probe drop test model was statically more stable in pitch than expected from wind tunnel tests. This is believed to be due to different spin vane incidence and small changes in the separation pattern over the ramp and drag plates, which contribute importantly to the static stability.

Acknowledgments

A number of individuals who were then students in the Department of Aerospace Engineering at the University of Kansas contributed importantly to the design of the drop models, conduct of the tests, and initial reduction of the data. These include Howard Henry, Douglas Carlson, Steven Erickson, and Michael Griswold. Thanks also are due to our colleague Donn B. Kirk for a careful review and constructive comments on this paper.

References

[1] Seiff, A., Kirk, D.B., Young, R.E., Blanchard, R.C., Findlay, J.T., Kelly, G.M., and Sommer, S.C., "Measurements of Thermal Structure and Thermal Contrasts in the Atmosphere of Venus and Related Dynamical Observations: Results from the Four Pioneer Venus Probes," *Journal of Geophysical Research*, Vol. 85, Dec. 30, 1980, pp. 7903-7933.

[2] Sorensen, T.C. and Muirhead, V.U., "Wind Tunnel Investigation of Low-Speed Buffeting of the Pioneer Venus Probes," *Journal of Spacecraft and Rockets*, Vol. 15, Jan.-Feb. 1978, pp. 34-39.

[3] Muirhead, V.U., "Investigation of Probe Buffeting Problem at Low Subsonic Mach Numbers," University of Kansas Flight Research Laboratory Report 500, University of Kansas, Lawrence, Kansas, July 1975.

[4] Seiff, A., Reese, D.E., Sommer, S.C., Kirk, D.B., Whiting, E.E., and Niemann, H.B., "PAET, An Entry Probe Experiment in the Earth's Atmosphere," *Icarus*, Vol. 18, April 1973, pp. 525-563.

[5] Brooks, J.D., "Some Anomalies Observed in Wind-Tunnel Tests of a Blunt Body at Transonic and Supersonic Speeds," NASA TN D-8237, June 1976.

[6] Oswald, T.W., "Pioneer Venus Large Probe Pressure Vessel Aerodynamics, Final Report," Hughes Aircraft Company Contract Report HS 507, Hughes Aircraft Company, Segundo, Calif., Oct. 1976.

[7] Blanchard, R.C. and Phillips, W.P., "Comparisons of Subsonic Drag Estimates Derived from Pioneer Venus Probes Flight Data with Wind-Tunnel Tests," Paper 80-1578 presented at the AIAA 7th Atmospheric Flight Mechanics Conference, Aug. 11, 1980.

[8] Johnson, D.B., Barker, E.H., and Lowe, P.R., "A Numerical Study of Fog Clearing by Helicopter Downwash," *Journal of Applied Meterology*, Vol. 14, Oct. 1975, pp. 1284-1289.

[9] Muirhead, V.U., "Pioneer Venus Probe Models Instrumented Drop Tests," University of Kansas Flight Research Laboratory Report 333-1, University of Kansas, Lawrence, Kansas, Aug. 1978.

[10] Counselman, C.C., Gourevitch, S.A., King, R.W., Loriot, G.B., and Ginsburg, E.S., "Zonal and Meridional Circulation of the Lower Atmosphere of Venus Determined by Radio Interferometry," *Journal of Geophysical Research*, Vol. 85, Dec. 30, 1980, pp. 8026-8030.